

Investigation of Fluid-Structure Interaction of a Submerged Steel Cylinder

Hamed Valaei^{1*}, Javad Moradloo²

1. M.Sc Student, School of Engineering, Department of Civil Engineering, University of Zanjan
2. Assistant Professor, School of Engineering, Department of Civil Engineering, University of Zanjan

ARTICLE INFO

Article history:

Received: 7 May 2023

Accepted: 9 May 2023

Keywords:

*Dynamic Response
Fluid-Structure Interaction,
Finite element analysis
Steel Cylinder*

ABSTRACT

Fluid-structure interaction (FSI) is a complex and critical field of study with a range of practical applications in the underwater domain. The present study investigates the FSI effect on two submerged steel structures consisting of ring-stiffened cylinders. The cylinder structures and the surrounding water are modeled using shell and acoustic finite elements, respectively. The study focuses on the dynamic response of the structures when subjected to an acoustic pressure shock wave. The results of the analysis, including the displacement and strain experienced by the structures, are presented and compared. This study provides valuable insights into the FSI effect on submerged structures, which has important implications for a wide range of applications. The findings of this study can contribute to the development of robust and efficient designs for submerged structures that can withstand the harsh underwater environments.

1. Introduction

The study of the interaction between fluids and structures is an important field of research, particularly in the engineering of submerged steel cylinders. The performance of these structures under extreme loading conditions, such as underwater shock loading, is of great interest to engineers. Fig.1 shows an example of the pressure hull. Researchers have studied the dynamic response of submerged steel cylinders subjected to simulated underwater shock waves. C.F.Hung, et al. [1] studied the linear and nonlinear dynamic responses of three cylindrical shell structures subjected to shock wave in a 4m × 4m × 4m water tank. Both end of the cylindrical shell were mounted with thick plates

to provide support and enclosed space. The three cylindrical shells were differently stiffened. The plastic deformation of the cylindrical shell was observed at a standoff distance of less than 50 cm. Dynamic analyses were performed for the experimental model using FEM and compared with the empirical test results. The accelerations and dynamic strains of cylindrical shells obtained from experiment were compared with those obtained by FE analysis.

C.Y. Jen [2] optimized geometrical model of a cylindrical structure and modeled the cylinder subjected to shock wave according to that geometry. Results of this study can be used in optimized design of stiffened pressure hull structures. Y.W. Kwon and P.K.Fox [3] studied the nonlinear dynamic response of a cylinder subjected to a far-field shock wave using both numerical and experimental models. Both ends of the cylinder were closed with thick flat plates. Strains at different locations of the structure were compared in experimental and numerical methods. Generally comparison of the two methods was satisfactory. This study showed improvements of the numerical results compared to the experimental data. The numerical study indicated that the dynamic motion of the cylinder

*Corresponding author's email: hamed.valae@gmail.com

has an accordion mode, a breathing mode and a whipping mode.



Fig.1. Samples of submarines

2. Materials and Methods

2.1. Equations of shock wave

Shock wave problems on submerged structures can be categorized to near-field and far-field types. In the near-field problem distance between source and standoff point is less than maximum radius of produced gas bubble. Some phenomena are related to this event, including the direct shock wave, sea-surface and sea-bed reflected shock waves, local hull and bulk cavitation effects, and gas bubble pulsation and migration effects. Shockwave pressure is added to the hydrostatic pressure. The pressure-time variations initially start with Maximum Pressure (in time less than 10^{-7} second) and then decreases by exponential type curve. Cole [4] presented this relation by an empirical equation:

$$P(t) = P_{\max} e^{-(t/\lambda)}, \quad t \geq t_1 \tag{1}$$

Where P_{\max} is peak pressure at the shock front (Mpa), t is time elapsed since the shock arrived (s), and λ is the exponential time decay. The peak pressure and decay constant depend on the standoff distance at which pressure is measured. equations (2) and (3) are define by:

$$P_{\max} = k_1 \left(\frac{W^{1/3}}{R} \right)^{A_1} \text{ (MPa)} \tag{2}$$

$$\lambda = k_2 W^{1/3} \left(\frac{W^{1/3}}{R} \right)^{A_2} \text{ (ms)} \tag{3}$$

Where k_1 , k_2 , A_1 and A_2 are constants. The reflected pressure of shock wave from fluid-structure interaction surface can be accurately predicted

by using Taylor’s Plate theory [5]. By using Newton’s second law of motion:

$$m \cdot \frac{dv_p}{dt} = P_i + P_r \tag{4}$$

Where m : Mass per unit area (m) , P_i : Incident-plane shockwave , P_r : Reflection wave of pressure and v_p : Plate velocity

If the velocity of particles behind the incident wave is $v_i(t)$ and for reflected wave is $v_r(t)$ thus the velocity of plate is:

$$v_p(t) = v_i(t) - v_r(t) \tag{5}$$

Resultant pressure of incident and reflected wave can be calculated by $P_i = \rho_f c v_i$ and $P_r = \rho_f c v_r$ equations. Where ρ_f fluid density and c is the speed of sound in water. By using equations (1) and (4) :

$$P_r(t) = P_i(t) - \rho_f c v_p = P_{\max} e^{-t/\lambda} - \rho_f c v_p \tag{6}$$

Equation of motion can be written as:

$$m \cdot \frac{dv_p}{dt} + \rho_f c v_p = 2P_{\max} e^{-t/\lambda} \tag{7}$$

Equation (7) is a first-order linear differential equation and velocity of plate can be determined by solving it:

$$(8)$$

$$v_p = \frac{2P_{\max} \lambda}{m(1-\beta)} [e^{-\beta t/\lambda} - e^{-t/\lambda}]$$

$$\text{Where } \beta = \frac{\rho_f c \lambda}{m} \text{ and } t > 0.$$

Total pressure on the plate is equal to:

$$P_t(t) = 2P_i(t) - \rho_f c v_p = \frac{2P_{\max} \lambda}{(1-\beta)} [e^{-t/\lambda} - e^{-\beta t/\lambda}] \tag{9}$$

Total pressure will be negative by increasing β in equation (9). Local cavitation will be happen by

decreasing the total pressure to vapor pressure because water can resist tension. Energy of shockwave is equal

to:

$$E = \frac{1}{\rho_f c} \int_0^{6.7\lambda} P(t)^2 dt \tag{10}$$

$$E = \frac{P^2_{max} \lambda}{2\rho_f c} \tag{11}$$

and almost equal to:

$$E \approx 89 \times 10^3 \cdot \frac{W}{R^2} \tag{12}$$

The magnitude of the shockwave impulse depends on time integral of pressure in p-t diagram. The impulse of a unit area of a shockwave front up to time t after its arrival is given by [4] , [6] :

$$I = \int_0^t P(t) dt \tag{13}$$

2.2. Simulation and dynamic response analysis

In the present study dynamic analysis of two different stiffened cylindrical shell subjected to shock wave pressure were presented. Ends of the cylinders are hemispherical and the stiffeners are T shape. First cylinder has 23 stiffeners and second stiffened by 11 ones as shown on Fig.3. The cylinders are located at 3.66 m depth of water and the source of shock wave is located at 7.62 m distance from middle of structure. Fig.2 shows locations of cylinder and source. Geometry of cylinders is presented in Table 2.

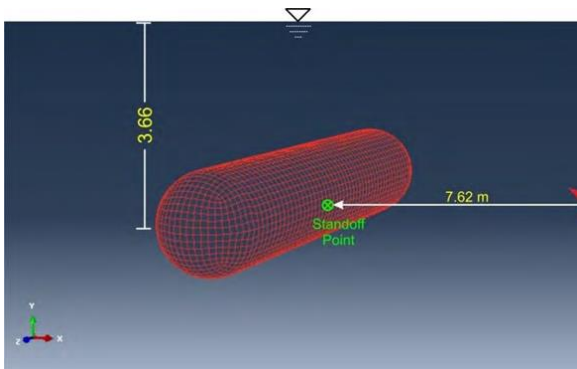


Fig.2. Schematic presentation of the cylinder

Table 2. Geometry of cylinders

| | |
|--|---|
| Cylinder Radius = 0.1525 m | Length of cylindrical section= 1.067 m |
| Radius of hemispherical ends = 0.1525 m | Shell thickness= 1.305 mm |

Surrounding fluid model contains 2 important parts: middle cylindrical section and hemispherical ends. Radius of cylinder and hemispherical ends are 0.915 m.

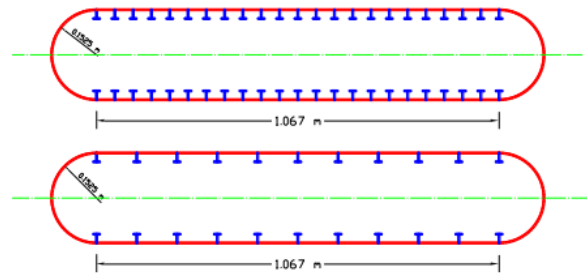


Fig.3. Section of cylinders (top: 23 stiffened down:11 stiffened)

Cylindrical structure was meshed shell elements (Fig. 4) and surrounding fluid meshed by solid elements(Fig. 5).

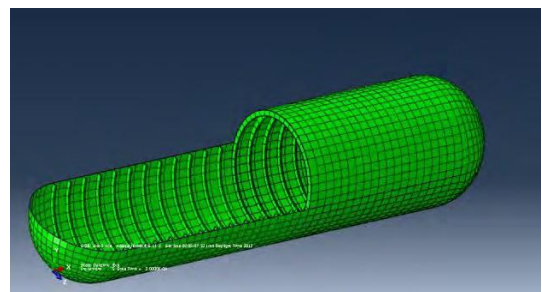
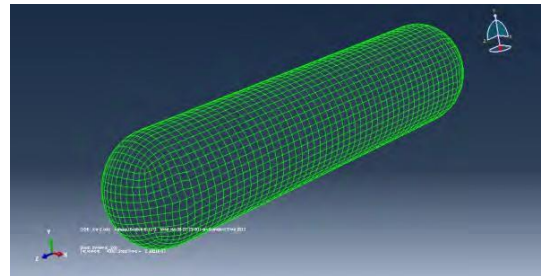


Fig.4. Finite element model of cylinder

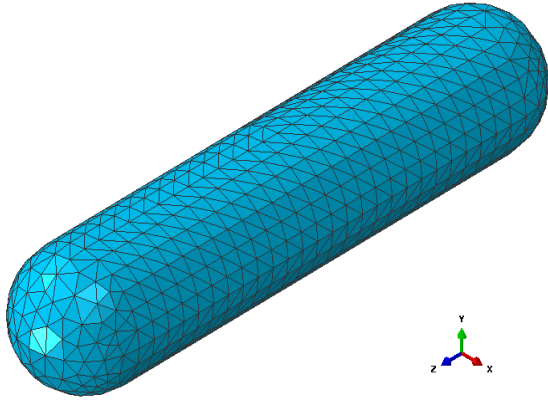


Fig.5.Finite element model of surrounding fluid

Fluid and cylinder instances assembled as shown on Fig. 6. The source of shock wave is located on 7.62 distance of standoff point according to X coordinate.

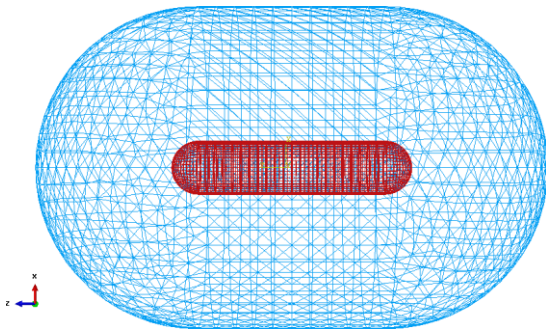


Fig.6.Assembling cylinder in surrounding fluid

In this study the fluid-structure interaction was defined between outer surface of cylinder and inner surface of surrounding fluid. Outer surface of fluid was defined as non-reflective boundary. According to (1), (2) and (3) equations, Table 3 contains the necessary magnitude of parameters to define the pressure load of the shock wave.

Table 3.Loading Properties

| | |
|-------------------------------------|------------------|
| Peak pressure of shock wave (Pmax): | 15.72 MPa |
| Distance (R): | 7.62 m |
| Time decay constant(λ): | 0.308 ms |

Considered analysis time duration is equal to 8 ms. Fig. 7 shows exponential Pressure-Time loading curve.

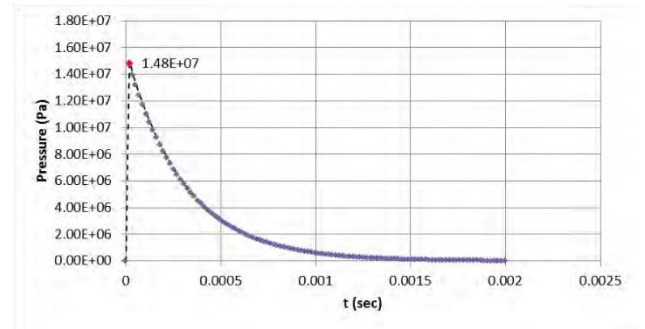


Fig.7.Pressure vs. Time loading curve

2.3. Coupled fluid-structure interaction equation

Interaction analysis should be performed for determining response of cylinders subjected to shock wave. Steel cylinder affected by the loading will be deformed and move surrounding water. Pressure distribution on cylinder depends on movements of the cylinder. The interaction between the fluid and the structure that exists until the vibration of the system has decayed has to be modeled using coupled fluid- structure equations. A surface-based procedure was used to enforce a coupling between the structural surfacenodes and the fluid surface nodes. The reflections of the pressure wave after striking the structure are called scattered waves, which needed to be taken into account while solving the finite element equations. Therefore, the applied load used for solving the finite element equations consisted of the sum of known incident and unknown scattered pressure wave components. The equations of motion used in this analysis are of the form [9] :

$$M_s \ddot{u} + C_s \dot{u} + K_s u = -[S_{fs}]^T p \quad (14)$$

$$M_f \ddot{p} + C_f \dot{p} + K_f p = [S_{fs}]^T T \quad (15)$$

$$P = P_I + P_s \quad (16)$$

Where M_s is the structural mass, C_s is the structural damping matrix, K_s is the structural stiffness matrix, P_I is the incident shock pressure wave, and P_s is the scattered pressure wave. In the above equations, u is the structural

displacements, M_f is the mass of fluid, C_f is the fluid damping matrix, K_f is the fluid stiffness matrix, and the transformation matrix S_f integrates the fluid and structural degrees of freedoms and was defined on all of the interacting fluid and structural surfaces. The fluid traction T is the quantity that describes the mechanism by which the fluid drives the solid. Fig. 8 shows interaction between Fluid and Structure, Fluid surface as Master and structural surface as Slave.

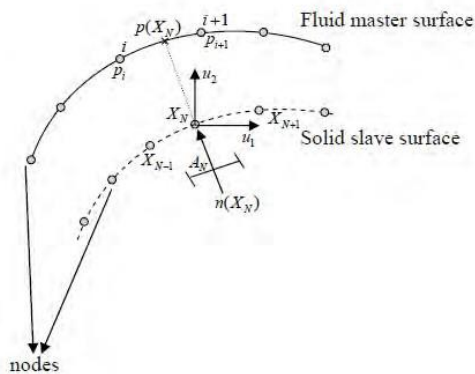


Fig.8. Master and Slave surfaces of Fluid-Structure interaction

3. Results and discussions

Consider “Model 1” title for 11 stiffened cylinder and “Model 2” title for 23 stiffened cylinder. Deformations caused by shock wave are shown in Fig.9 and Fig. 10 at 2 and 8 (ms) time after shock wave. Accordion and breathing deformations of Model1 is more than Model 2. Deformation scale factor was set to 20 for better view.

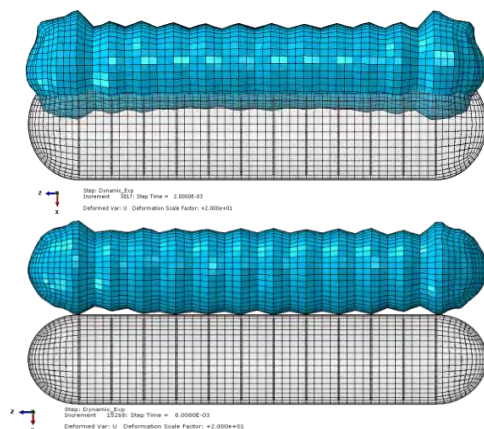


Fig.9. Deformation of Model 1 (11 stiffened cylinder, Scale factor=20)

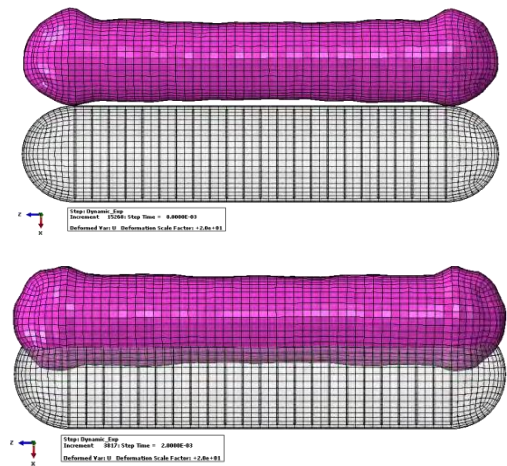


Fig.10. Deformation of Model 2 (23 stiffened cylinder, Scale factor=20)

Three important points located on the each cylinder were considered for better investigation of deformation curves. Two points were located on the ends of the cylinder and one standoff point was located on middle of cylinder length which is the nearest point to the source. As shown in Fig. 11 displacement curves of the end points are almost coincided in each cylinder but displacement of the standoff point is different from endpoints in early duration. Red curve shows the displacements of the standoff point. According to Fig. 11, displacements of the three points in every cylinder were almost 15 mm at 8 ms time after analysis.

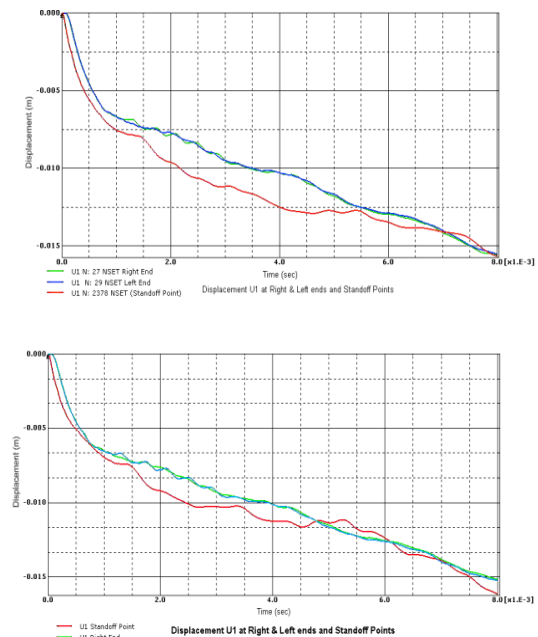


Fig.11. Displacement of endpoints and standoff point. (Right: 23 stiffened Left: 11 stiffened)

Four points have been chosen on perimeter of the lateral section in the half length of the cylinders and equivalent plastic strain has been investigated on them. According to Fig. 12, Point B3 had maximum equivalent plastic strain (PEEQ) but the magnitude for Model1 was more than Model2.

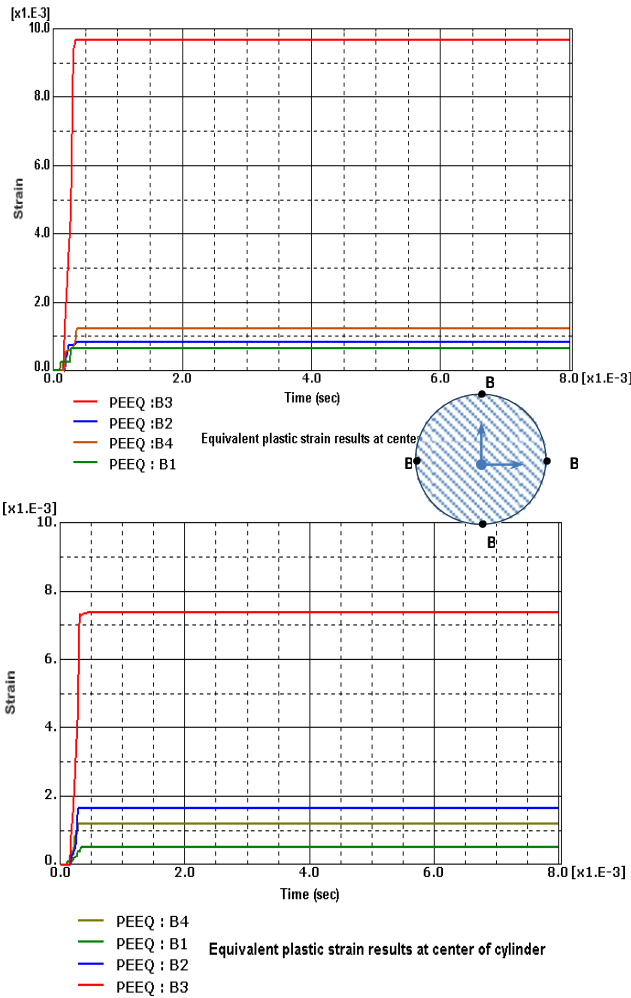


Fig.12.Equivalent plastic strain at 4 nodes on perimeter of the section. (Right: 23 stiffened Left: 11 stiffened)

4. Conclusion

In this study dynamic analysis of two submerged steel cylinders with different stiffened array subjected to shock wave is presented. Some important nodes of the structure were chosen for investigating the responses of the two models. Results showed that accordion and breathing deformation of cylinder stiffened by 23 T shape stiffener is less than other which stiffened by 11 ones nonetheless the displacement of each cylinder was almost the same magnitude of 15 mm at time of 8 ms.

If we consider side of cylinders opposed to shock wave and other side of them, results showed that standoff point (B1) had minimum PEEQ in other hand Point (B3) had maximum magnitude of PEEQ. Thus it's obvious that B3 needs more stiffen. Results of this study can be used in better design of storage and pressure hulls and their stiffeners pattern.

5. References

1. C.F. Hung, B.J. Lin, J.J. Hwang-Fuu, P.Y. Hsu, Dynamic response of cylindrical shell structures subjected to shock wave, *Ocean Engineering*, Volume 36, Issue 8, June 2009, Pages 564–577
2. Y.W. Kwon, P.K. Fox, Underwater shock response of a cylinder subjected to a side-on loading, *Computers & Structures*, Volume 48, Issue 4, 17 August 1993, Pages 637–646
3. C.Y. Jen, Coupled acoustic–structural response of optimized ring-stiffened hull for scaled down submerged vehicle subject to underwater shock wave. *Theoret Appl Fract Mech* 2009; 52:96–110
4. R.H. Cole, Princeton University Press, Princeton, 1948
5. G.I. Taylor, The pressure and impulse of submarine shock waves on plates, *Compend. Underwater Explos. Res. ONR 1* (1950) 1155–1174.
6. R. Rajendran, K. Narasimhan, Deformation and fracture behaviors of plate specimens subjected to underwater shock wave – a review, *Int. J. Impact Eng.* 32 (2006) 1945–1963.
7. Liu G. R., Quek S.S. *The Finite Element Method*, National University of Singapore; 2003.
8. Roy T., Chakraborty D. *Delamination in Hybrid FRP Laminates under Low Velocity Impact*, Indian Institute of Technology; 2006.
9. Rajesh Kalavalapally, Ravi Penmetsa, Ramana Grandhi, *Multidisciplinary optimization of a lightweight torpedo structure subjected to an underwater shock wave*, *Finite Elements in Analysis and Design*, Vol.43, (2006), Pages 103 – 111.